ASSESSMENT OF THE GASFLOW SPRAY MODEL BASED ON THE CALCULATIONS OF THE TOSQAN EXPERIMENTS 101 AND 113

M. A. Movahed

AREVA GmbH Offenbach, Germany

J. R. Travis

FZK Research Centre Karlsruhe, Germany

Abstract

Within the framework of the EU (**E**uropean **U**nion) project SARNET (**S**evere **A**ccident **R**esearch **Net**work), spray experiments were performed in the TOSQAN facility in France. The experiments, Test 101 (thermal hydraulic part, without He release) and Test 113 (dynamic part, with He release), were selected for benchmark calculation with different CFD (**C**omputational **F**luid **D**ynamics) and LP (**L**umped **P**arameter) codes. The CFD participants performed their calculations with a 2D geometry of the TOSQAN vessel without considering the pre-steam injection phase, but using the average values from the experiment for the simulation of the initial condition at the start of the spray.

AREVA performed two GASFLOW post-test analyses of the Test 101 with the full 3D geometry simulation of the vessel:

- **Part simulation (PS)**: without considering the pre-steam injection phase, but using the average values from the experiment for the simulation of the initial flow conditions at the start of the spray.
- **Full simulation (FS)**: considering the pre-steam injection phase resulting in determination of the initial flow conditions at the start of the spray.

FZK performed 2D calculations simulating the spray injection phase with and without He release in Tests 101 and 113, respectively. Furthermore FZK simulated the pre pressurization of the vessel with He in Test 113.

The calculations of the TOSQAN spray experiments were necessary for validating the GASFLOW spray model because the effect of sprays on hydrogen risk had been investigated with this code for different LOCA (**L**oss **o**f **C**oolant **A**ccident) events, with and without delayed depressurization resulting in fast homogenization of the EPR™ containment atmosphere.

The comparison of the calculations with the measured experimental results showed good agreement between calculation and measurements for Test 101 in all four phases; namely, vaporization phase, fast condensation phase, and slow condensation phase, as well as the equilibrium phase. Furthermore, it showed the same tendency for fast homogenization of the vessel atmosphere as mentioned above in the spray calculation for the EPR™. The comparison showed maximum deviations of only about 3% for all three global values; namely, pressure, gas mean temperature, and gas mole number. Simulation of Test 113 showed less then 6% deviation for the He volume concentration after 250 s spray time while the He stratification is fully destroyed as was seen in the experiment.

The selected mesh or control volumes for TOSQAN geometry provides an extrapolation from the compared results to prototypic containment scale. The linear scale of the TOSQAN vessel relative to the EPR™ nuclear power plant is about 1:22.

The GASFLOW code is a finite volume computer code, which has been developed at the Los Alamos National Laboratory in USA and the research centre Karlsruhe in Germany. The code is designed to be a best-estimate tool for predicting the transport of steam/hydrogen/air mixtures, with/without spray, as well as the recombination and combustion of hydrogen with the possibility of adding other gases for simulating design basis or severe accidents in nuclear reactor containments. GASFLOW models are validated with numerous experiments describing different thermohydraulic phenomena in the

containment. These simulation analyses have shown that the GASFLOW spray model is applicable and reliable for the containment analyses due to good agreement with experimental results and can be applied for simulating all relevant phases during spraying, particularly during the thermodynamic equilibrium phase with and without light gas release.

1. INTRODUCTION

The EPR™ power plant is equipped with a two train spray system for maintaining the containment pressure below its design value and to avoid failure of the containment by over-pressurization in case of severe accident. It minimizes the leakage rate to the annulus, as may result from long-term steam production caused by decay heat removal from the melt; either in the spreading room, or in case of arrested core degradation, in the reactor pressure vessel. Thus, the numerical simulation of the spray system is necessary for the assessment and prediction of the atmospheric composition as well as the impact on possible hydrogen combustion modes during its action.

In accident events with core degradation, hydrogen can be produced in considerable amounts and released into the containment. Although the installed auto-catalytic recombiners in the containment remove significant amounts of hydrogen in the long term, the accumulation of hydrogen in the short term can not be avoided, and a combustible mixture can form.

After spray system actuation, steam in the containment atmosphere condenses on cold droplet surfaces flowing from the spray nozzles. Consequently, the steam volume concentration is reduced resulting in an increase of the hydrogen/air/steam mixture sensitivity with respect to combustibility. On the other hand, due to the high density of the droplets flowing in the upper part of the containment, strong convection flows will be initiated and established. Hence an effective fast homogenization of the atmosphere can occur with continuous reduction of hydrogen mass due to the action of the auto-catalytic recombiners.

Thus, there is a competition (in terms of gas mixture ignition) between steam condensation, with increased hydrogen risk, and atmosphere homogenization and hydrogen removal, with a decreased hydrogen risk. Therefore, the French Authorities have requested AREVA to demonstrate that early operation of the spray system will not interfere with hydrogen risk. To demonstrate that the operation of the spray system will not interfere with hydrogen risk, the GASFLOW CFD code (Travis et al. 2007) has been used to determine the hydrogen distribution and removal, as well as for the assessment of combustion modes in the containment for the licensing of the EPR™. The effect of sprays on hydrogen risk has been investigated with the GASFLOW code among others for a bounding scenario 20 cm^2 small break LOCA with delayed depressurization. The spray system is actuated at an unfavorable moment when high amounts of hydrogen accumulate in the containment (Movahed et al. 2003). The calculations show fast homogenization of the EPR™ containment atmosphere associated with decreasing hydrogen risk.

In the framework of the EU project SARNET, spray experiments were performed in the French TOSQAN facility (Malet et al. 2006). TOSQAN experiments 101 and 113 were selected for benchmark calculations with both CFD and LP codes. The CFD participants performed their calculations on a 2D axial-symmetric geometry.

AREVA participated in the EU project SARNET by performing post-test calculations of the TOSQAN experiment 101 with the same code parameters as was used in the GASFLOW assessment for spray impact on hydrogen risk in the EPR™. The initial and boundary conditions of the TOSQAN experiment were fully accounted for in the 3D geometry simulation of the vessel. FZK also participated in the project and performed pre and post-test calculations for both Tests 101 and 113 with a 2D geometry simulation of the vessel during the spray phase and He release.

This paper describes the results of the AREVA and FZK analyses for the TOSQAN Tests 101 and 113, respectively, and compares the results of the calculations with the experimental results and assesses the spray model in GASFLOW for the determination of the impact of sprays on hydrogen risk.

2. GASFLOW CODE

GASFLOW is a finite-volume computer code that was developed at the Los Alamos National Laboratory in USA and FZK in Germany (Travis et al. 2007). The code is designed to be a best-estimate tool for predicting the transport of steam/H_2/air mixture as well as for the recombination and combustion of hydrogen with the possibility of adding other gases for simulating design base or severe accidents in containment of nuclear power plant. The prediction of the mixture quality is achieved by solving the transient, three-dimensional, compressible Navier-Stokes equations with multi-component gas mixtures. The code can model geometrically complex facilities with multiple compartments and internal structures in a multi-block computational domain. One-dimensional complex ventilation systems can be included to couple the multi-block capability. GASFLOW solves transport equations in Cartesian or cylindrical coordinates for multiple component gas mixtures using the k-ε, k-ω or an algebraic turbulence model.

GASFLOW predicts pressure and temperature developments during the course of an event, distribution of the specified gas species, stratification of the gas species, removal (recombination and burning) of combustible gases (hydrogen and carbon monoxide), heat and mass transfer to the structure/film, heat and mass transfer to the droplets, formation of mist, natural and forced convection flows, gas diffusion between neighboring cells, release of decay heat in the atmosphere (according to input), heating and cooling of the atmosphere, heating and cooling of the sump, leakage flow to environment, jet formation, spray simulation, formation of the water film on the structure surfaces and its transportation to the sump, collection of the condensate in a sump, thermal radiation, turbulence, and buoyancy effects.

The thermo-chemical properties are extracted from JANAF tables, and the transport properties are derived from the data base of the CHEMKIN code.

2.1 GASFLOW Spray Model

GASFLOW has an applicable and reliable spray model for containment analysis with the use of separate temperatures for gases and droplets. This model assumes a mechanical equilibrium between the phases (equal velocities for gas and droplets) and allows for thermal non-equilibrium between the phases (non-equal temperatures of gas and droplets). In particular, this means separate specific internal energy equations are applied for the liquid and gas phases. The pressure field is determined only from the gaseous components, while convective heat and mass transfer are modeled between liquid and vapor components to obtain appropriate coupling phenomena. Droplet depletion is modeled to provide the effect of liquid sinks from the fluid field resulting in droplet sedimentation or rainout and droplet-wall interaction. This model is similar to the model developed by CEA (**C**ommissariat à l'**E**nergie **A**tomique) for the CASTEM code (Caroli, 2000) with the assumption of the mechanical equilibrium.

Users can define the spray nozzle locations on the GASFLOW mesh. In addition, the spray water temperature, the effective diameter of the droplets, the spray water mass flow rate along with the direction of the spray jet (simultaneous injections of the spray water in all directions are possible) must be defined. Normally the area of the GASFLOW mesh faced to the spray nozzle is much larger than the actual nozzle diameter. Therefore, the droplet jet velocity is higher than the calculated droplet velocity close to the spray nozzle resulting in a broad droplet jet with small velocity close to the spray mesh. This means that the momentum of the droplet jet is neglected close to the nozzle opening. This is acceptable because the droplet velocity reduces rapidly from the jet velocity at the nozzle opening to the gas velocity over a few meters distance. Furthermore, due to the high density of the droplet flow close to the spray nozzle, the gravitational body force is dominate for initiating and establishing effective convection flows which transport the droplets to lower elevations below the spray nozzle.

2.2 Experimental Background and GASFLOW Code Validation

The available experimental facilities vary from small shock tubes up to full containment facilities like the HDR (Heiβdampf-Reaktor) in Karlstein Germany. It is not the intention of this paper to present a comprehensive overview of all the related facilities and experiments, rather some recent and important large scale experiments will be identified. Many experimental tests have been performed in the HDR

facility. The most important experiments for hydrogen distribution and mixing are the E11.2 and E11.4 experiments, which had simulated the high and low hydrogen and steam release location, respectively. The results showed clear stratification or homogenization of the atmosphere depending upon the release position (high or low). FZK participated in the ISP-47 program using the GASFLOW code for pre- and post-test calculations for specified experiments in the TOSQAN, MISTRA and THAI test facilities. Some of the objectives of these International Standard Problems are: code comparisons between predictions and experimental transients, identifying and decreasing codes deficiencies, reducing the uncertainties of the codes, and finally improvement of the quality of the assessment of the relevant safety issues.

Large numbers of pre- and post-test calculations with GASFLOW have been performed over many years showing good agreement with the observed steam and hydrogen distributions.

The following Table 1 summarizes the key phenomena and experiments for GASFLOW validation.

Table 1: Some of the experiments applied for the GASFLOW models validation

Phenomena	**Experiments**
Steam/hydrogen transport	HDR T31.5; Battelle Rx4, Rx5; Phebus FPT0; Phebus hydraulic tests; HDR E11.2
Steam inertization	Battelle Gx7
Helium jet injection	Battelle Hyjet Jy7
Hydrogen recombination	Battelle Gx4, Gx6, Gx7; Battelle MC3
Hydrogen combustion, igniters	HDR E12; Battelle HX; FZK tube; Battelle Gx7; Bureau of Mines tests; SNL Flame experiment
Steam condensation	ThAI 7 (blind calculation); ThAI 1 (open calculation), ThAI 7 (blind calculation); MISTRA (MICOCO exercise)
He/steam distribution	ThAI 10 (blind calculation); TOSQAN (blind calculation)
Spray	TOSQAN 101 (steam test); TOSQAN 113 (He test); MISTRA MASPn (steam test), MARC2B (He test)

3 SIMULATION

These sub-chapters describe briefly the EPR^{TM} containment and TOSQAN vessel geometry with a delineation and outline of the main features, relevant differences, and similarities between them.

3.1 EPR^{TM} Containment Geometry Delineation

The GASFLOW CFD code has been applied to computationally validate the hydrogen control system in the EPR^{TM}. The containment volume of about 80000 m^3 is subdivided in a cylindrical coordinate mesh with 30 control volumes in the radial direction, 69 control volumes in vertical direction and 60 control volumes in azimuthal direction for a total number of 124,200 control volumes. The computational cells were uniformly spaced in the azimuthal direction (6º) (see Fig. 1). The inclusion of internal structures, containment shell with steel liner, plus all features relevant for the assessment of the hydrogen concept have been modeled (e.g. spray system and recombiners as well as the CONVECT system for making the EPR^{TM} containment partly accessible for safe maintenance working condition during plant operation and which ensures in case of accident global and local convection flow).

This detailed nodalization of the containment geometry is indispensable, since the influence of structures, components, doors, grids, and openings have considerable impact on the gas transport and mixing as well as on the turbulence generation and combustion processes. The water reservoir IRWST (**I**n-Containment **R**efueling **W**ater **S**torage **T**ank) is located in the lower part of the containment. This water is available for different purposes such as core melt cooling in the spreading area in case of a severe accident or for suction of the spray system. Also the steam condensate on structures during a LOCA scenario will be collected in the IRWST.

3.2 TOSQAN Vessel Geometry Delineation and Experimental Procedure

Fig. 2 (left side 2 plots) shows a sketch and an instrumentation arrangement for the TOSQAN facility. The vessel boundary consists of double thin steel walls with oil circulated in the gap. The gap is sub-divided into different sections. The temperature of the wall can be controlled by circulating oil in different sections with different temperatures (Malet et al., 2006). The vessel volume is about 7 m^3 with the internal diameter and the height equaling 1.5 m and 4.8 m, respectively. A pot is located in the lower part of the TOSQAN vessel. The condensate can be collected in the pot and removed through a drain line. The spray nozzle can be moved along the central vertical axis, which allows experimental measurements under different conditions. Fig. 2 (2 right side plots) shows the mesh for the GASFLOW 3D and 2D simulations, respectively.

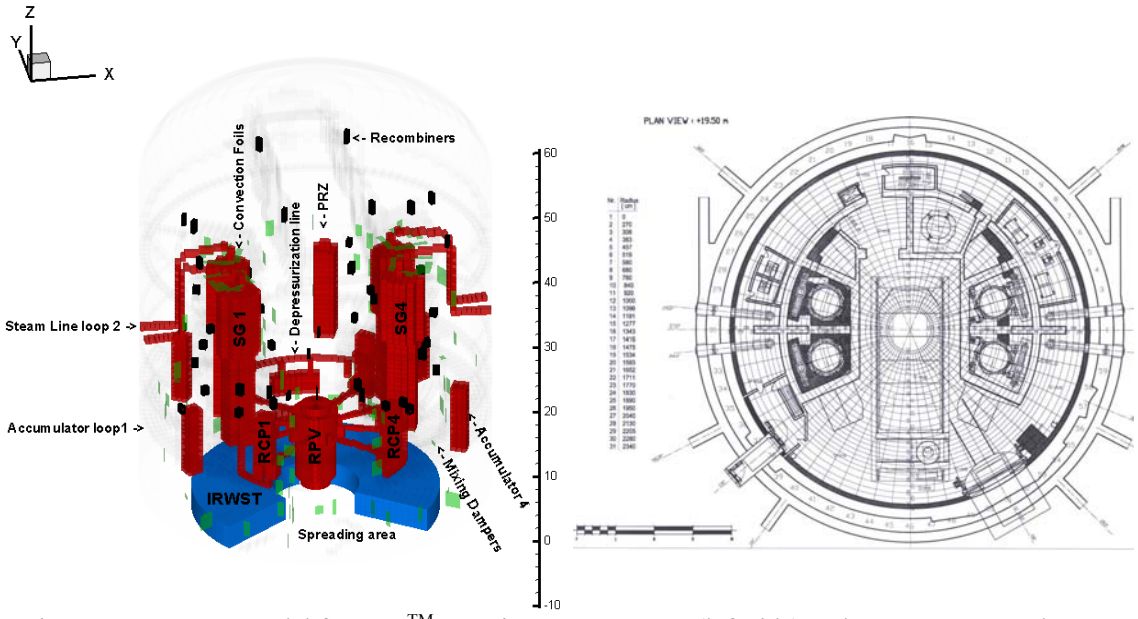

Fig. 1: GASFLOW model for EPR™ containment geometry (left side) and GASFLOW mesh cross section at level +19.50 m (right side).

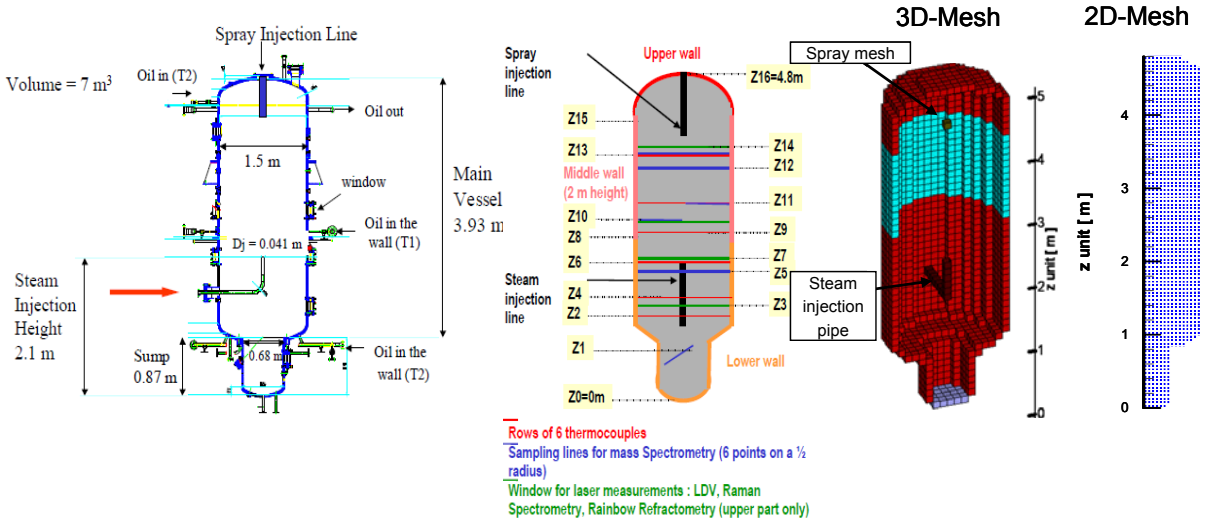

Fig. 2: Sketch of the TOSQAN facility and the instrumentation (left side 2 plots) and GASFLOW 3D and 2D geometry (right side 2 plots).

In the 3D simulation, the vessel volume is subdivided in a regular Cartesian coordinate system with 10 cm cubes. 15x15 control volumes were used in horizontal plane, while 48 control volumes were used

in the vertical direction for a total number of 10,800 computational volumes. In the 2D simulation, a square mesh size of 5 cm was used resulting in 1,440 control volumes.

The location of the spray nozzle, the air/steam/He injection pipe, and the sump floor can be seen in the TOSQAN vessel sketch and the corresponding GASFLOW 3D geometry representation. The selected 10 cm cube volumes in a regular Cartesian coordinate system has the advantage of representing the spray nozzle with one cell exactly along the central axis (similar to the use of one control volume for simulating a spray nozzle in the EPR™ analyses), and at least five horizontal computational cells applied to the sump area, which allows possible counter current flow in the pot, while sub-dividing the vessel diameter in exactly 15 control volumes. The 3D simulation of the vessel allows the simulation of the steam injection pipe which results in a small non-symmetrical flow field. Comparison of the local parameters can be provided at the exact position of the corresponding measurement points.

In Test 101, super-heated steam is injected into the vessel (initially air at 1 bar pressure) from a boiler at 8 bar through an aperture of regulation valves. The steam is throttled from 171.4ºC (8 bar) to 145ºC and 151ºC at 1 bar and 2.5 bar as the vessel pressurizes. The steam mass flow rate is about 13 g/s. The wall temperatures were controlled by heated oil circulations and measured. The measured wall temperatures are used as boundary conditions from the start of spraying up to the end of the test. Table 2 shows the measured mean wall temperatures of each section for the time after the injection of the super-heated steam.

The total numbers of moles were determined at the start of spraying to be 213 and 308 for air and steam, respectively, which corresponds to a steam volume fraction of 59.1%. The flow rate of spray water was 30 g/s with a temperature of 119.1ºC at t = 0 s, 22.1ºC at 311 s and 22.7ºC from 1000 s to the end of the test. The water temperature during the evaporation phase is required to correctly predict the pressure and temperature development. The pressure at the initiation of spraying was 2.5 bar and the gas temperature was between 130.0ºC close to the spray zone and 131.1ºC elsewhere, while the droplet size was 145 μm and the spray angle was 55º in both tests.

Table 2: TOSQAN Test 101: Measured wall temperatures

Time [s]	Mean wall temperature [ºC]	Upper wall temperature [ºC]	Middle wall temperature [ºC]	Lower wall temperature [ºC]
Just before spray injection	122.1	121.8	122.3	121.7
0 - 102	121.5	121.4	121.6	121.3
107 – 300	120.4	120.8	120.4	120.3
306 – 601	119.9	120.3	120.0	119.4
End of the test	118.9	119.3	120.1	115.4

In Test 113, initially air at 1 bar, He is injected radially with a flow rate of 1 g/s until the pressure is 2 bar. The distribution/stratification was measured with a mass spectrometer and indicated a uniform profile along the radius. After a 400 s delay, spraying was activated with cold water at 30ºC and a mass flow rate of 30 g/s. The outer boundary walls were only insulated and not controlled (Malet et al., 2006). Droplet size was 137 μm. Table 3 shows the measured mean gas temperature and He volume concentration at different levels at spray activation. The test condition (no steam) in the vessel is not similar to the EPR™ containment during relevant events for spraying because there steam is always present. FZK simulated the He injection phase.

Table 3: TOSQAN Test 113: Initial condition at the start of spray water injection

Level Z (from bottom) [m]	Helium concentration [vol%]	Mean gas temperature [ºC]
Z13 = 3.93 m	99.0 ± 0.5	31.8
Z11 = 3.135 m	85.8 ± 0.5	36.9
Z10 = 2.8 m	47.6 ± 1.0	at Z9 = 2.675 m: 34.72
Z5 = 1.9 m	2.3 ± 0.5	at Z6 = 2.045 m:30.13
Z1 = 0.87 m	1.9 ± 0.5	at Z2 = 1.210 m: 28.70

The size of the mesh for these calculations must be sufficiently large to ensure the applicability of comparing the simulations and experiment with the assessment of the EPR™ spray analysis. On the other hand, the mesh must be small enough to resolve all relevant phenomena occurring during the experiment. Fig 3 shows the GASFLOW 3D mesh scaling between the EPR™ analysis and the TOSQAN Test 101 simulation. This figure exhibits also the second root of the ratio of the control volume surfaces (perpendicular to the three coordinate directions) and third root of the ratio of the control volume, spray mass flow rate and containment/vessel volume which are of the same order of magnitude as the other ratios of the relevant geometry parameters.

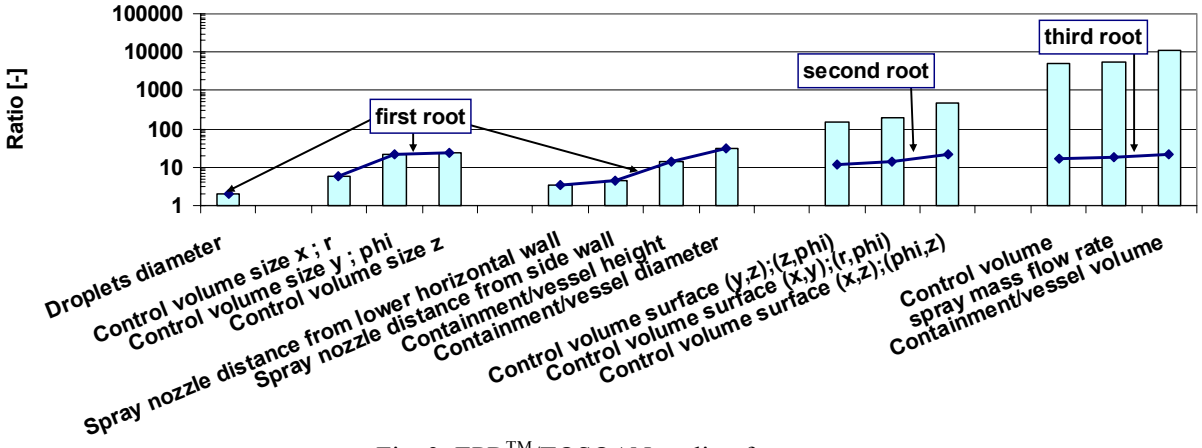

Fig. 3: EPR™/TOSQAN scaling factors.

The data for determining the ratio between spray analysis in the EPR™ and the TOSQAN experiments is the respective control volume sizes. It should be mentioned that all computational volumes used for EPR™ analyses have a similar shape (hexahedral mesh) except those at the center. As mentioned before, all control volumes in the TOSQAN Test 101 calculations are cubes and have the same size. Scaling factors for different parameters and length scales between EPR™ and TOSQAN analyses are of the same order of magnitude. The choice of the 10 cm cubes for the TOSQAN calculations results in proper scaling factors for all significant geometry parameters between 3.4 and 31.2.

Since the scaling factors for significant geometry parameters are within an acceptable order of magnitude, the results of the comparison between TOSQAN experimental results and GASFLOW calculations are applicable for the EPR™ GASFLOW analyses. The linear scale of the TOSQAN

vessel relative to the EPR ™ nuclear power plant is about 1:22 in comparison to the average scaling factor from all parameters of about 1:15.

4 EXPERIMENTAL RESULTS AND PERFORMED CALCULATIONS

The discussion of the global and local results is now presented separately for each test.

4.1 Thermal Hydraulic Part: Test 101

Figs. 4 to 6 show the comparison of the time history for three global values: pressure, average gas temperature and gas mole number in the TOSQAN vessel for the two calculations PS (part simulation) and FS (full simulation). The comparison of the calculations with the measured experimental results shows good agreement in all four phases; namely, vaporization phase, fast condensation phase, slow condensation phase, and in the equilibrium phase. The comparison shows maximum deviations of about 3% for all three global values which occur during the evaporation phase. The lack of sufficient experimental information for adequately describing the pre-steam injection phase and spray water temperature history is apparent.

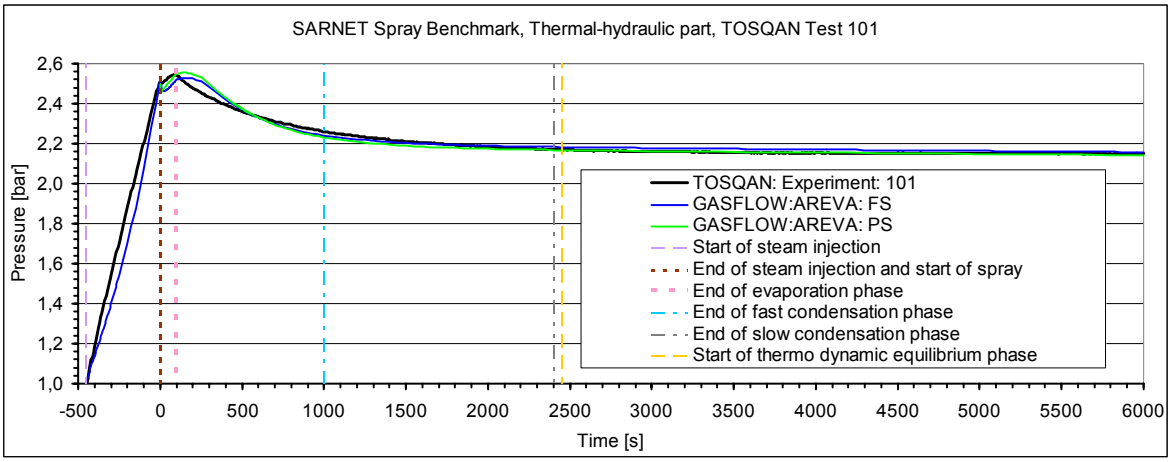

Fig. 4: TOSQAN Test 101: Comparison of the absolute pressure

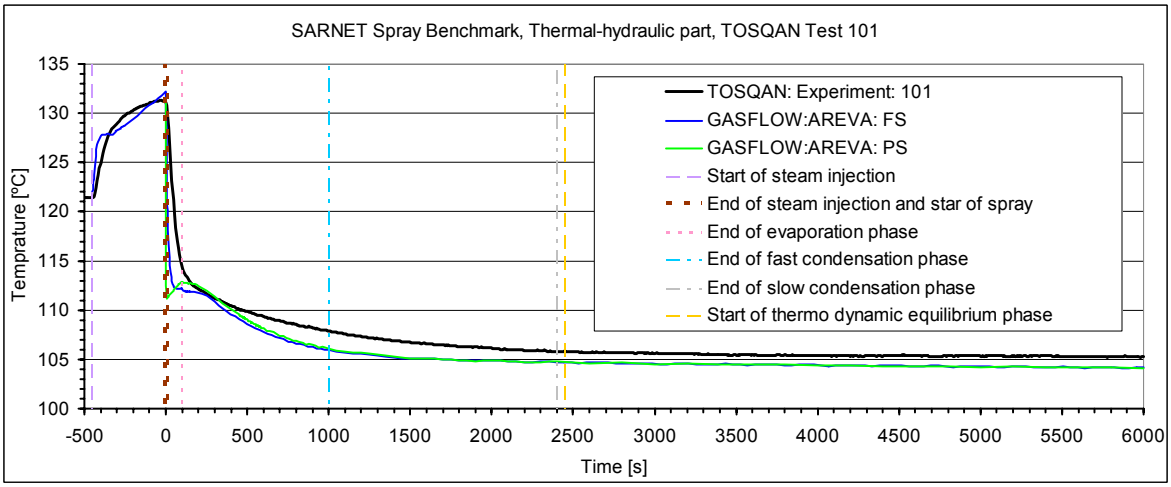

Fig. 5: TOSQAN Test 101: Comparison of the average gas temperature

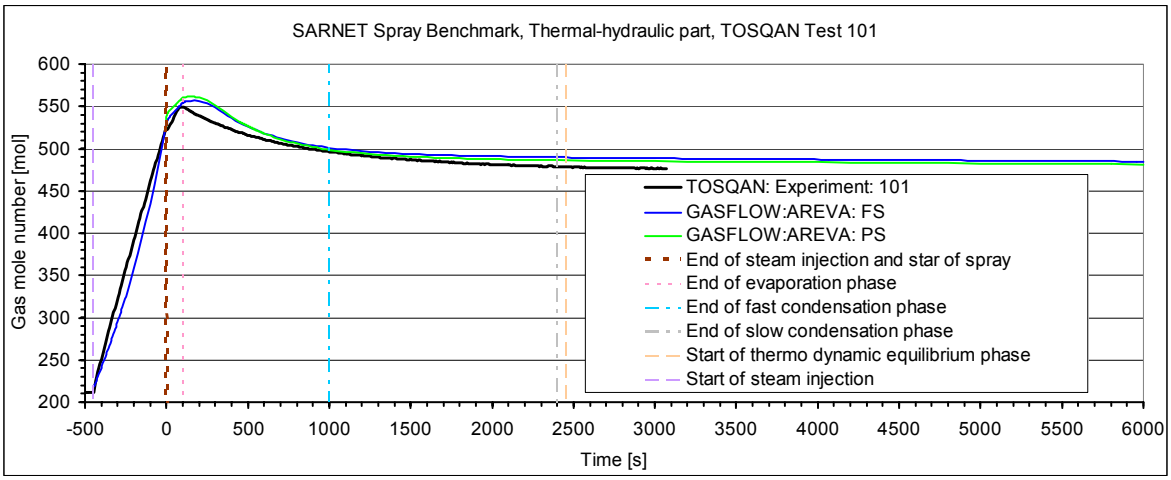

Fig. 6: TOSQAN Test 101: Comparison of the gas mole number

Figs. 7 to 8 and 9 to 10 show the local radial gas temperature profiles below the spray nozzle (Z14) and at a lower location in the vessel (Z6, above the pot) at times of 600 s and 6000 s, respectively. The comparison shows very good agreement outside the vicinity of spray nozzle. The deviation close to the location below the spray nozzle on the central axis indicates the insufficient resolution of the spray flow area with one computational volume. This inaccuracy close to the spray nozzle head has no impact on the determination of the flow variables elsewhere as can be seen in figures that present the local variable (Figs. 7 to 15).

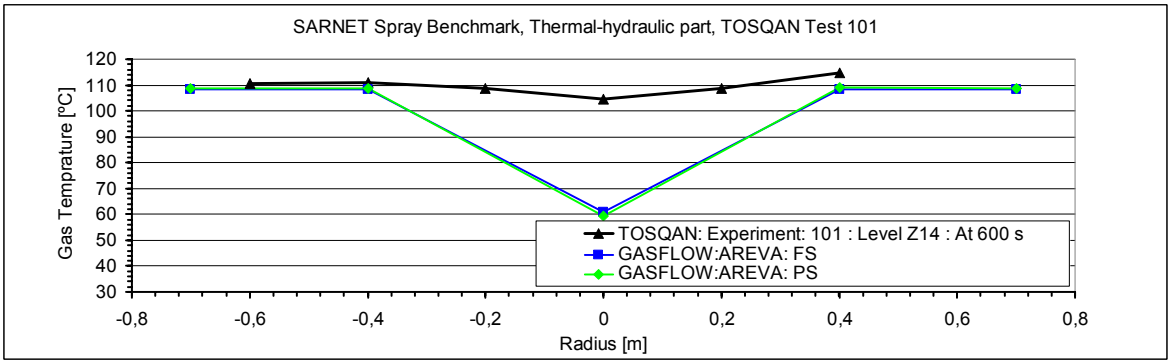

Fig. 7: TOSQAN Test 101: Gas temperature, radial profile on the level Z14 at t = 600 s

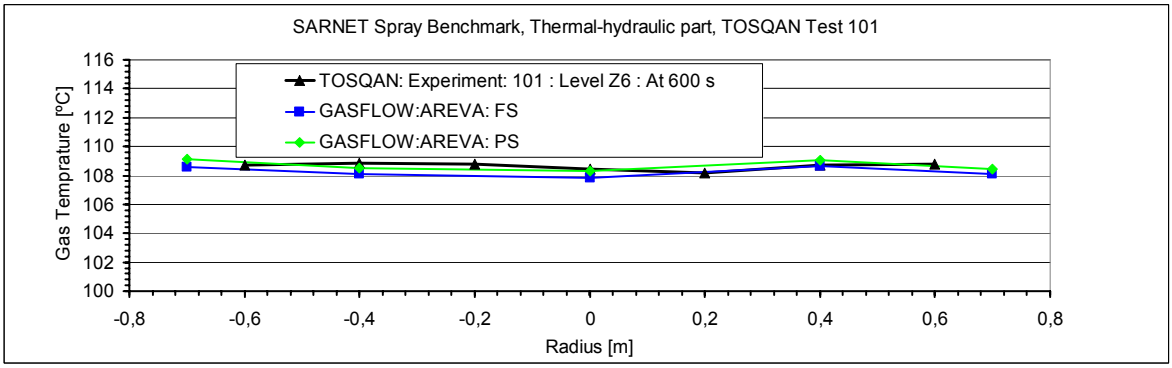

Fig. 8: TOSQAN Test 101: Gas temperature, radial profile on the level Z6 at t = 600 s

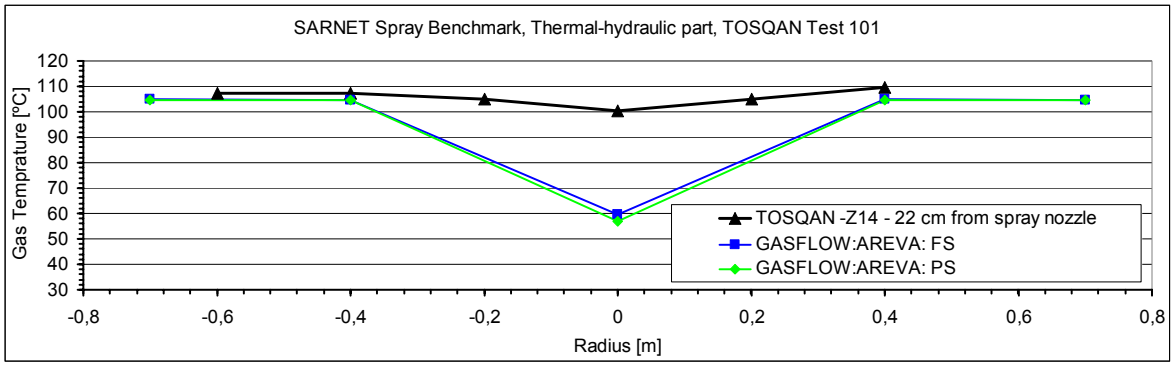

Fig. 9: TOSQAN Test 101: Gas temperature, radial profile on the level Z14 at t = 6000 s

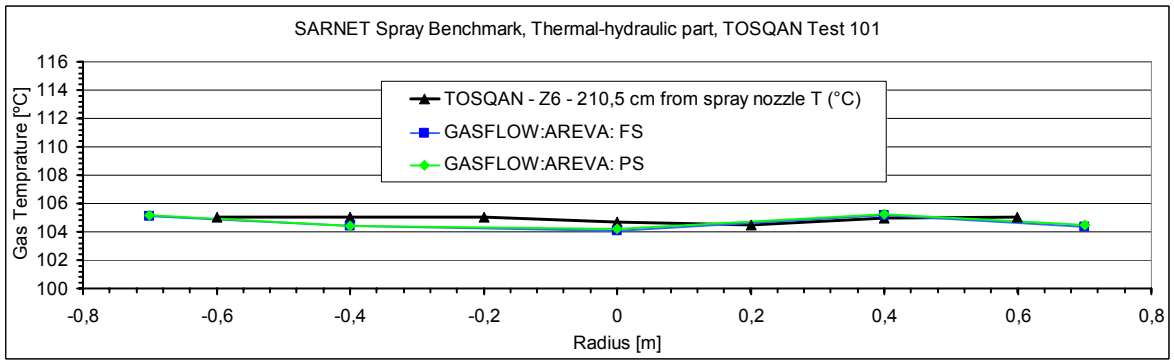

Fig. 10: TOSQAN Test 101: Gas temperature, radial profile on the level Z6 at t = 6000 s

Figs. 11 and 12 show the local vertical gas temperature profiles on the central axis, R12, and at the radius R = 0.296 m, respectively, at t = 6000 s during the equilibrium phase. In these figures, the location of the spray nozzle is indicated. The comparison exhibits the same behavior as was seen in the radial profiles.

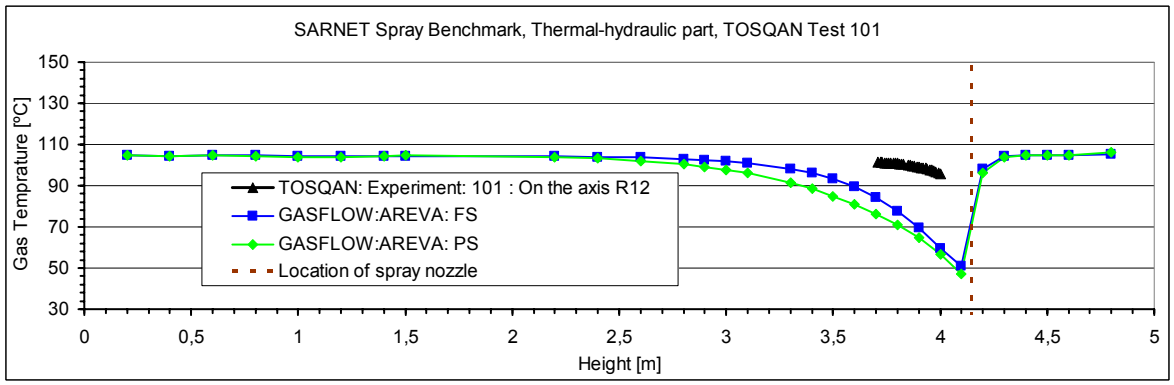

Fig. 11: TOSQAN Test 101: Gas temperature, vertical profile on the central axis of the vessel at t = 6000 s

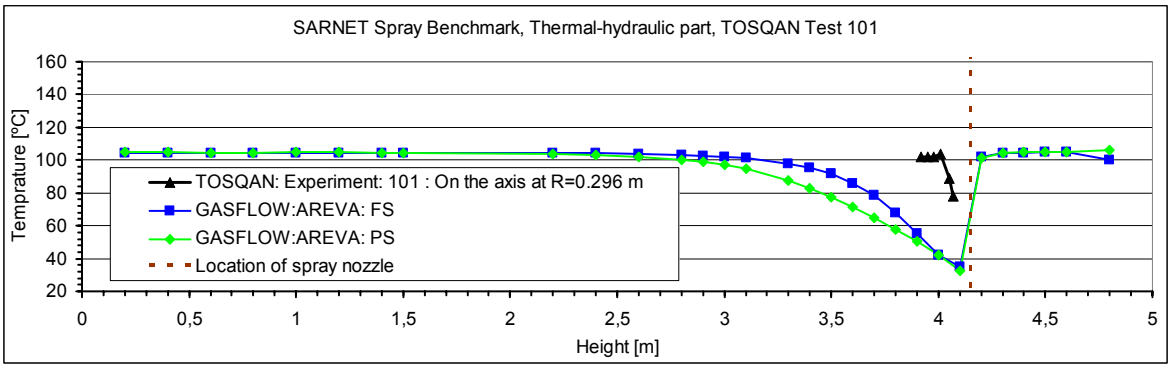

Fig. 12: TOSQAN Test 101: Gas temperature, vertical profile on the axis at radius R = 0.298 m near central axis at t = 6000 s

Figs. 13 and 14 show the local radial steam volume concentration profiles below the spray nozzle (Z14) and in lower part of the vessel (Z5, above the pot), respectively, at, t = 6000 s during the equilibrium phase. For the same time, Fig. 15 displays the local vertical steam volume concentration profiles close to the central axis R11 at a radius R = 0.1 m. The comparison yields very good agreement outside the vicinity of the spray nozzle. The deviation close to the spray nozzle is explained on the one hand as before for the gas temperatures on the other hand the measurement with the mass spectrometry Mass sp. 180106 at 3.91 m shows in Figs. 13 very good agreement between calculated and measured data at radius 0.7 m near vessel wall just below the level of the spray nozzle. This measurement shows the same deviation as the calculation with others measurement like Ramman sp 261004 at 4 m (R = -0.67 m) which indicates some uncertainty of the experimental data.

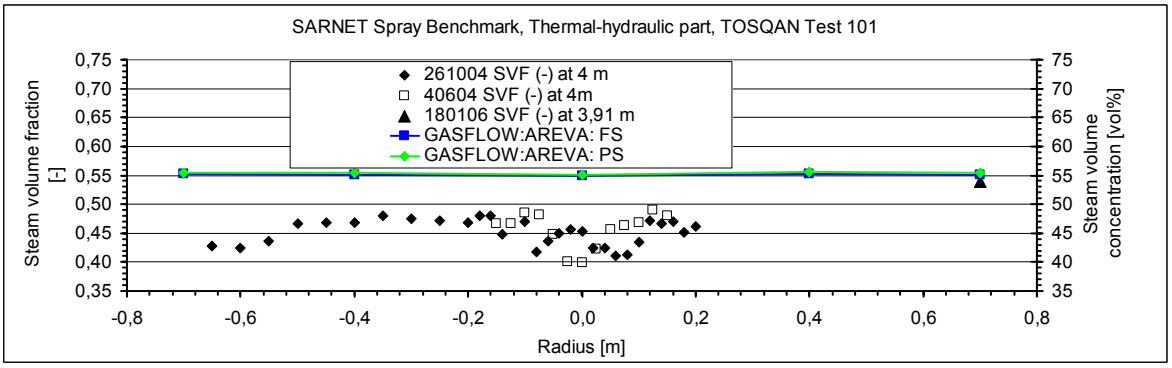

Fig. 13: TOSQAN Test 101: Steam volume fraction radial profile on the level Z14 at t = 6000 s

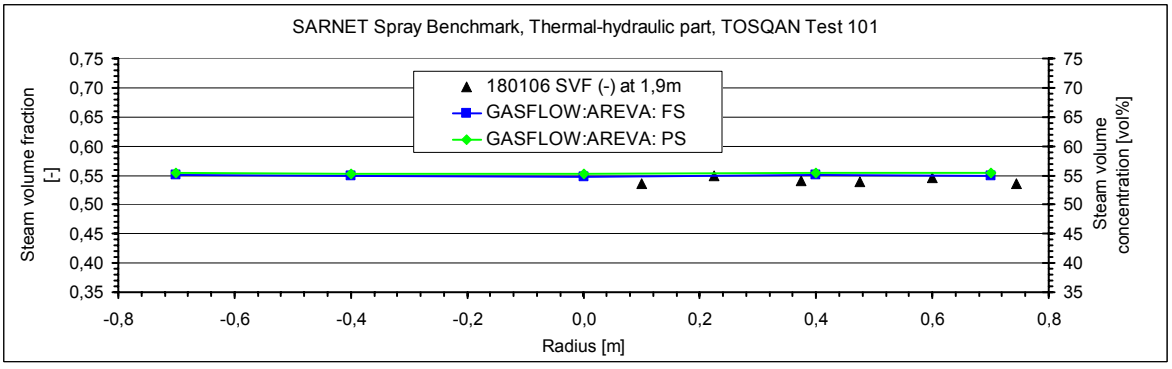

Fig. 14: TOSQAN Test 101: Steam volume fraction radial, profile on the level Z5 at t = 6000 s

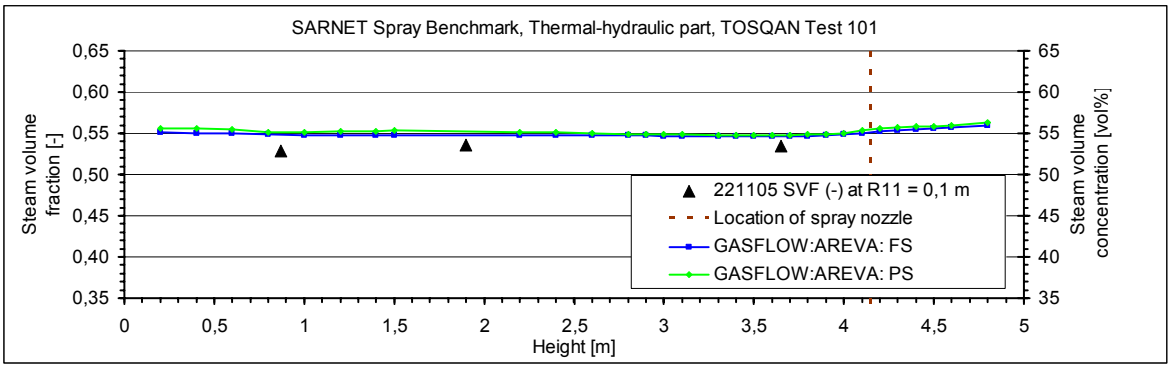

Fig. 15: TOSQAN Test 101: Steam volume fraction, vertical profile close to the axis of the vessel at t = 6000 s

4.2 Dynamic Part: Test 113

Fig. 16 shows the comparison of two global values, pressure and average gas temperature, in the TOSQAN vessel Test 113. The calculated and measured experimental results show good agreement after global mixing is reached (after about t = 250 s). The comparison exhibits maximum deviations of about 3% for these two global values. This occurs during the He stratification break-up phase and when the global gas mixing is reached for temperature and pressure, respectively.

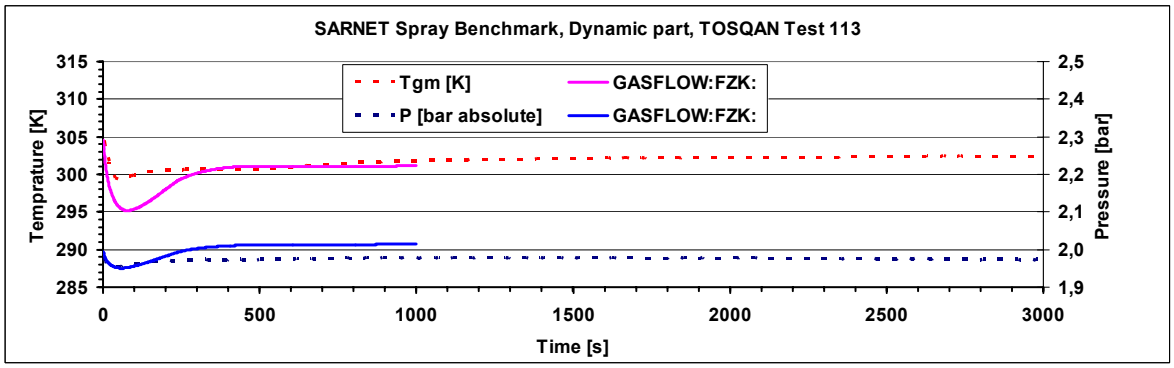

Fig. 16: TOSQAN Test 113: History of the absolute pressure and gas temperature

Fig. 17 shows the local vertical He volume fraction profiles on the axis, R8, at half of the TOSQAN vessel radius for different times. In this figure, the location of the spray nozzle and He injection nozzles are indicated. The comparison shows very good agreement between calculation and measurement throughout the experiment.

Fig. 18 shows at the time t = 1000 s (after global gas mixing was reached at about t = 250 s) the local radial He volume concentration profiles below the spray nozzle (Z13; 22 cm below the spray nozzle) and in the upper part of the pot (Z1; in the sump area). The comparison demonstrates very good agreement outside the vicinity of spray nozzle. The deviation close to the location below the spray nozzle is explained by the same reasoning as mentioned for the gas temperature.

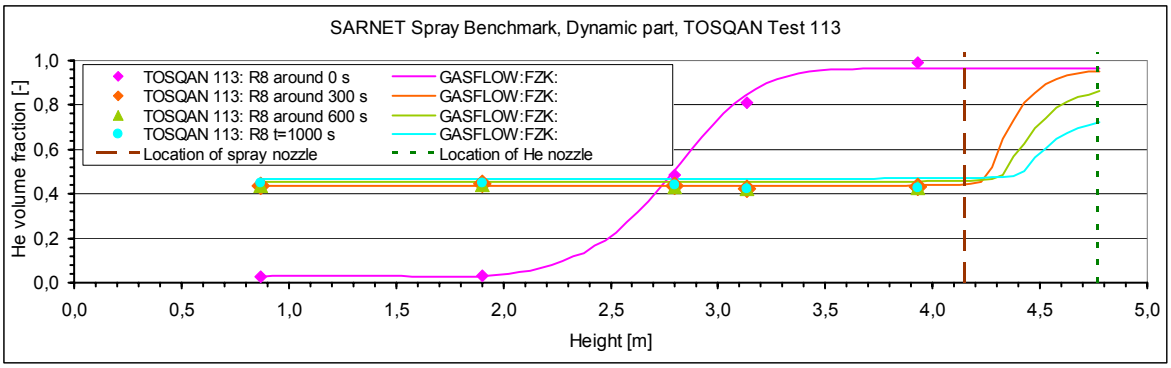

Fig. 17: TOSQAN Test 113: He fraction, vertical profile on the axis between centre and wall of the vessel at different times

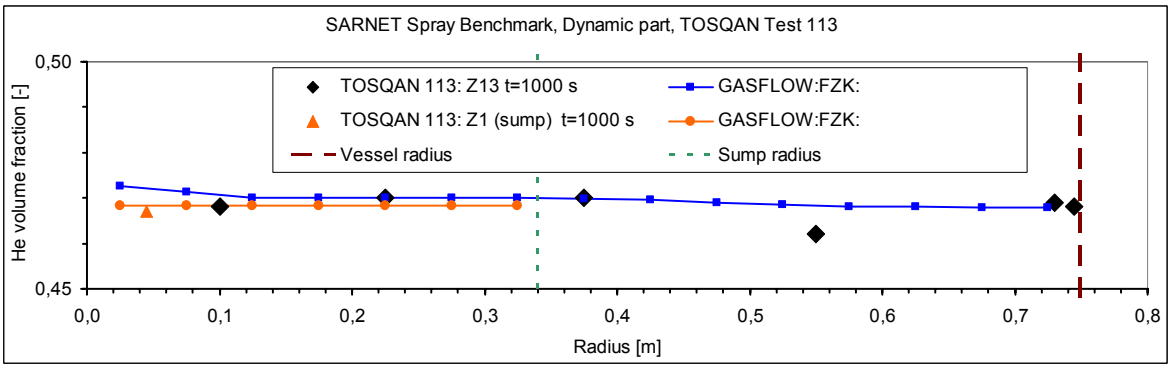

Fig. 18: TOSQAN Test 113: He volume fraction, radial profile below the spray nozzle (Z13) and in the sump (Z1) at t = 1000 s

Fig. 19 shows the time history of the local He volume fractions at different levels located on the axis R8, at half TOSQAN radius. For the He break-up phase, the comparison is sufficient; particularly, since the initial conditions at spray activation display up to 5.5 vol% deviation from the measurement in the central region of the vessel due to insufficient resolution of the complex He injection system which releases He in a horizontal level. The absolute errors at the time of activation of the spray are about -2.6 vol%, 3.2 vol%, 5.5 vol%, -0.2 vol% and -0.3 vol% at levels Z13, Z11, Z10, Z5 and Z1, respectively. This simulation shows less then 6% deviation in the He volume concentrations after 250 s spray time.

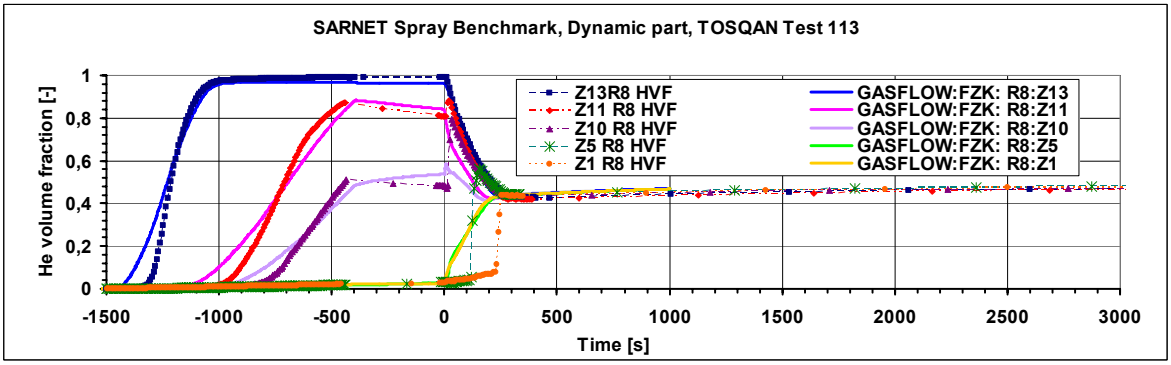

Fig. 19: TOSQAN Test 113: History of He volume fraction in different levels on the axis between centre and wall of the vessel (0: time of spray actuation)

The comparison shows sufficient agreement in all three phases namely during the He injection phase and around the time of spray activation as well as after the break up phase taking into account the impossible proper delineation of the complex He injection system with the selected mesh size to ensure the applicability of comparing the simulations and experiment with containment spray analyses.

5 CONCLUSION

The TOSQAN experiments 101 (thermal hydraulic test without He release) and 113 (dynamic part with He release) were simulated with the GASFLOW CFD code. AREVA performed two post-test analyses of the experiment 101 with a full 3D geometry of the vessel. FZK performed pre- and post-test analyses for both tests in a 2D geometry. The FZK analysis of Test 101 is without considering the pre-steam injection phase, but the analysis of Test 113 takes into account the He release phase before spray activation. Calculations considering the pre-steam/He injection phase have the advantage of calculating the initial conditions at the time of spray activation.

These analyses of the TOSQAN spray tests are useful for validating the GASFLOW spray model to ensure the effects of spraying on the hydrogen risk are adequately simulated and investigated for severe accidents.

Comparison of the calculated results with measurements show good agreement for Test 101 in all four phases; namely, vaporization phase, fast condensation phase, slow condensation phase, and equilibrium phase (around 3% deviation). For Test 113, the agreement is good for the phase after global gas mixing is reached. The comparison shows maximum deviations of about 3% for both global values which occur during the He stratification break-up phase and when the global gas mixing is reached for temperature and pressure, respectively. For the He break-up phase, the comparison is sufficient; particularly, since the initial conditions at spray activation display up to 5.5 vol% deviation from the measurement in the central region of the vessel due to insufficient resolution of the complex He injection system. Furthermore, the tests show the same tendency for fast homogenization of the atmosphere as mentioned above for the spray calculations of the EPR™.

The mesh resolution provides an extrapolation for the results to prototypic containment scale. The linear scale of the TOSQAN experiment relative to the EPR™ nuclear power plant is about 1:22. The reliability and applicability of the GASFLOW spray model is demonstrated with good agreement between simulation and experiment for the TOSQAN Tests 101 (steam test) and 113 (He test).

REFERENCES

J.R. Travis, J.W. Spore, P. Royl, et al., ”GASFLOW - A computational Fluid Dynamics Code for Gases, Aerosols and Combustion” Report LA-13357-M and FZK-5994, Vol I-III, Oct. (2007).

M.A. Movahed, J. Eyink, J.R. Travis, “Effect of Spray Activation on the Reactivity of the Hydrogen-Air-Steam Mixture in The Containment of the EPR™“ *NURETH-10* Seoul, Korea, Oct. 5-9, (2003).

J. Malet, E. Porcheron, J. Vendel, L. Blumenfeld, I. Tkatschenko “SARNET Spray Benchmarks TOSQAN and MISTRA” *Specification Report Rev. 1 DSU/SERAC/LEMAC/06-11* May (2006).

C. Caroli “Modeling of Spray in the Reactor Containment during a Severe Accident” *Rapport DMT SEMT/LTMF/RT/00-016/A* Oct. 26 (2000).

J. Malet, P. Metier, “SARNET Spray Benchmark TOSQAN Thermal Hydraulic Part Test 101 Code Experiment Comparison Report ” *Ref. DSU/SERAC/LEMAC/07-03* December (2007).

J. Malet, J. Vizet, “SARNET Spray Benchmark TOSQAN Dynamic Part Test 113 Code Experiment Comparison” *Ref. DSU/SERAC/LEMAC/08-04* April (2008).